



ELSEVIER

Journal of Power Sources 97–98 (2001) 303–307

JOURNAL OF  
**POWER  
SOURCES**

www.elsevier.com/locate/jpowsour

# Synthesis of $\text{LiAl}_y\text{Co}_{1-y}\text{O}_2$ using acrylic acid and its electrochemical properties for Li rechargeable batteries

Won-Sub Yoon, Kyung-Keun Lee, Kwang-Bum Kim\*

*Division of Materials Science & Engineering, Yonsei University, 134 Shinchon-dong, Seodaemun-gu, Seoul 120-749, South Korea*

Received 18 July 2000; accepted 4 December 2000

## Abstract

The structure and electrochemical properties of  $\text{LiAl}_y\text{Co}_{1-y}\text{O}_2$  cathodes for Li rechargeable batteries have been closely examined by neutron diffraction, X-ray diffraction (XRD), X-ray absorption spectroscopy (XAS), differential scanning calorimetry (DSC), and electrochemical methods. Neutron diffraction patterns and Co K-edge X-ray absorption near-edge structure (XANES) spectra of  $\text{LiAl}_{0.25}\text{Co}_{0.75}\text{O}_2$  revealed that aluminum and cobalt ions were statistically distributed in octahedral 3b sites of the ordered  $\alpha\text{-NaFeO}_2$  structure. The DSC scan of  $\text{Li}_{0.5}\text{Al}_{0.25}\text{Co}_{0.75}\text{O}_2$  showed an increase in the peak temperature and reduction in the exothermic peak compared to those of  $\text{Li}_{0.5}\text{CoO}_2$ , and it indicates that Al-doped  $\text{LiCoO}_2$  shows the good thermal stability of the cathode and reduction of the heat of reaction. © 2001 Elsevier Science B.V. All rights reserved.

*Keywords:* Sol-gel process;  $\text{LiAl}_y\text{Co}_{1-y}\text{O}_2$ ; Lithium rechargeable batteries; XANES

## 1. Introduction

$\text{LiCoO}_2$  is the most promising material for its technological use as cathodes of Li rechargeable batteries because lithium ions are electrochemically intercalated and deintercalated with high reversibility [1–3]. One of the modifications to improve its electrode performance is to substitute Co with metal ions which may stabilize the layered structure with or without participating in the redox processes [4–6]. As aluminum is both lighter and less expensive than cobalt, Al-doped  $\text{LiCoO}_2$  could be a cheaper and lighter cathode material than the pure  $\text{LiCoO}_2$ .

It has been reported that Al-doping is potentially attractive to electrochemical application since Al-doped  $\text{LiCoO}_2$  has advantages such as higher intercalation voltage, higher energy density, and a lower cost although it shows large capacity fading during cycling [7]. Tirado and co-workers reported with their X-ray diffraction (XRD) Rietveld analysis that a poor lithium ion diffusivity, resulting from the presence of aluminum in both tetrahedral and octahedral sites, may also be one of the reasons for the large capacity fading of Al-doped  $\text{LiCoO}_2$  cathode [4].

The performance of electrode materials is highly affected by their synthesis processes. Considerable improvements have been made by using a solution method in obtaining high performance cathode materials. Among the solution methods, sol-gel method makes possible a better mixing of the elements and therefore, a better reactivity of the mixture, which then allows a lower reaction temperature and a shorter reaction time. Additionally, the resulting powders also show good stoichiometric control and narrow particle size distribution [8–10]. In this study,  $\text{LiAl}_y\text{Co}_{1-y}\text{O}_2$  powders were synthesized using acrylic acid as a chelating agent. The structure and its electrochemical properties were studied by neutron diffraction, XRD, X-ray absorption spectroscopy (XAS), and electrochemical methods.

## 2. Experimental

$\text{LiAl}_y\text{Co}_{1-y}\text{O}_2$  powders were synthesized using acrylic acid as a chelating agent, as described in our previous work [11]. A stoichiometric amount of lithium acetate ( $\text{Li}(\text{CH}_3\text{COO})\cdot 2\text{H}_2\text{O}$ ), cobalt acetate ( $\text{Co}(\text{CH}_3\text{COO})_2\cdot 4\text{H}_2\text{O}$ ), and aluminum nitrate ( $\text{Al}(\text{NO}_3)_3\cdot 9\text{H}_2\text{O}$ ) with the cationic ratio of  $\text{Li}:(\text{Co} + \text{Al}) = 1:1$  was dissolved in distilled water and mixed with an aqueous solution of acrylic acid. Nitric acid was slowly added to the solution with constant stirring until a pH of 2 was achieved. The resulting solution was mixed

\* Corresponding author. Tel.: +82-2-361-2839; fax: +82-2-312-5375.

E-mail addresses: wonsuby@nownuri.net (W.-S. Yoon),  
kbkim@mail.yonsei.ac.kr (K.-B. Kim).

with a magnetic stirrer at 70–80°C for 6–8 h to obtain a clear viscous gel. The gel was dried in a vacuum oven at 100°C for 12 h. All the  $\text{LiAl}_y\text{Co}_{1-y}\text{O}_2$  compounds were ground and calcined at 800°C for 24 h after pre-calcining the obtained gel precursor at 400°C for 1 h in air.

The crystal structure of  $\text{LiCoO}_2$  calcined at various temperatures was characterized by XRD. Powder XRD pattern was recorded using an automated Rigaku powder diffractometer using Cu K $\alpha$  radiation. The neutron powder diffraction spectra were collected with a high-resolution powder diffractometer at the Korea Atomic Energy Research Institute. The wavelength, 1.8342 Å, was selected from the (3 3 1)-plane Ge monochromator. About 8 g of each sample was enclosed in a vanadium can (8 mm diameter). The 32 counters, spaced at five intervals, were moved by steps of 0.05° in the range  $0^\circ \leq 2\theta \leq 160^\circ$ . The neutron powder diffraction data were analyzed by the Rietveld profile analysis using the FULLPROF program [12,13]. EXAFS measurements were performed in transmission mode at beamline 3C1 of Pohang light source (PLS) using a Si(1 1 1) double-crystal monochromator. The storage ring was operated with an electron energy of 2 GeV and a current between 80 and 120 mA. Calibration was carried out prior to all measurements using the first inflection point of the spectrum of Co foil, i.e. Co K-edge = 7709 eV, as a reference.

Cathode specimens were prepared by mixing the  $\text{LiAl}_y\text{Co}_{1-y}\text{O}_2$  powders with 10 wt.% acetylene black and 6 wt.% poly-vinylidene fluoride (PVDF) in *n*-methyl pyrrolidone (NMP) solution. The mixture was spread on Al foil and pressed. The composite electrodes were dried under vacuum at 150°C for at least 12 h before use. A three-electrode electrochemical cell was employed for electrochemical measurements in which lithium foil was used for reference and counter electrodes. The electrolyte used was 1 M  $\text{LiClO}_4$  in propylene carbonate (PC) solution. All the electrochemical experiments were carried out at room temperature in a glove box filled with purified argon gas.

### 3. Results and discussion

XRD patterns of  $\text{LiAl}_y\text{Co}_{1-y}\text{O}_2$  calcined at 800°C for (a)  $y = 0$  and (b)  $y = 0.25$  are shown in Fig. 1. All diffraction lines can be indexed assuming a hexagonal lattice. The XRD pattern for  $\text{LiCoO}_2$  shows the good separations of the (0 0 6)/(0 1 2) and the (1 0 8)/(1 1 0) couples of diffraction lines, which indicates that this material is a well developed layered HT- $\text{LiCoO}_2$  [14]. As in the case of  $\text{LiCoO}_2$ , the XRD pattern for  $\text{LiAl}_{0.25}\text{Co}_{0.75}\text{O}_2$  shows that it has the same HT- $\text{LiCoO}_2$  structure. The separations of the (0 0 6)/(0 1 2) and the (1 0 8)/(1 1 0) couples of diffraction lines of  $\text{LiAl}_{0.25}\text{Co}_{0.75}\text{O}_2$  are wider than those of  $\text{LiCoO}_2$ .

The absorption peak features in the X-ray absorption near-edge structure (XANES) give useful structural information such as oxidation state of chemical species, site symmetry, and covalent bond strength. Fig. 2 shows normalized Co K-edge XANES spectra for  $\text{LiCoO}_2$  and  $\text{LiAl}_{0.25}\text{Co}_{0.75}\text{O}_2$ . The K-edge structures originate from transitions of the 1s core level of the metal to excited vacant states of proper symmetry involving metal orbitals. With adequate theoretical interpretation, each feature of XANES can be interpreted in terms of local geometry and local electronic structure [15–17]. The small pre-edge absorption, A peak, represents the transition of 1s electron to an unoccupied 3d orbital of  $\text{Co}^{3+}$  ion with the low spin ( $t_{2g}^6 e_g^0$ ) electronic configuration. Although the 1s  $\rightarrow$  3d transition is the electric dipole-forbidden transition in an ideal octahedral symmetry, the appearance of small absorption peak results from pure electric quadruple coupling and 3d–4p orbital mixing by the non-centrosymmetric environment of its slightly distorted  $\text{CoO}_6$  octahedral site. The first strong absorption, B peak, is assigned to a shakedown process involving the 1s  $\rightarrow$  4p transition with simultaneous ligand to metal charge transfer. The strongest absorption, C peak, is a pure 1s  $\rightarrow$  4p transition. As shown in Fig. 2, both the edge structures of  $\text{LiCoO}_2$  and  $\text{LiAl}_{0.25}\text{Co}_{0.75}\text{O}_2$  are identical, which indicates that introduction of Al into  $\text{LiCoO}_2$  structure does not cause

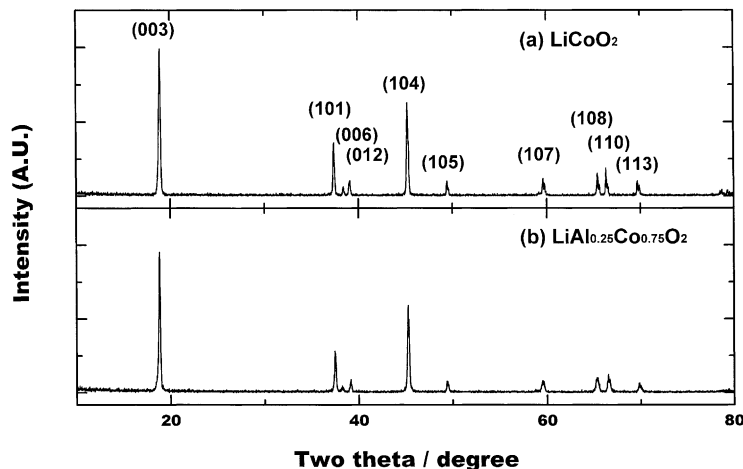


Fig. 1. XRD patterns for  $\text{LiAl}_y\text{Co}_{1-y}\text{O}_2$  calcined at 800°C for (a)  $y = 0$  and (b)  $y = 0.25$ .

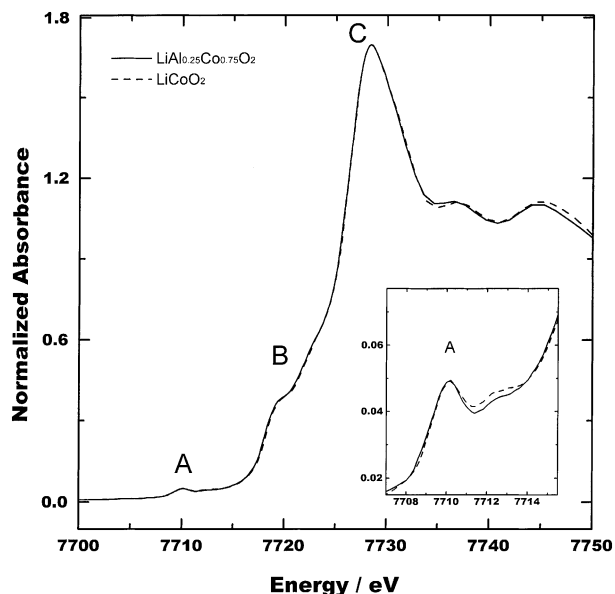


Fig. 2. Normalized Co K-edge XANES spectra for  $\text{LiCoO}_2$  and  $\text{LiAl}_{0.25}\text{Co}_{0.75}\text{O}_2$ . The inset shows an expanded view of the region of the spectrum containing the  $1s \rightarrow 3d$  transitions.

the change of local geometry and local electronic structure around Co atom.

$\text{LiCoO}_2$  and  $\text{LiAl}_{0.25}\text{Co}_{0.75}\text{O}_2$  electrodes were cycled at room temperature. The cells were charged from their rest potential up to 4.2 V for  $\text{LiCoO}_2$  and up to 4.3 V for  $\text{LiAl}_{0.25}\text{Co}_{0.75}\text{O}_2$ . Fig. 3 shows the first charge curves of  $\text{LiCoO}_2$  and  $\text{LiAl}_{0.25}\text{Co}_{0.75}\text{O}_2$  calcined at  $800^\circ\text{C}$  at a constant current rate of  $C/5$ . The  $\text{LiCoO}_2$  electrode calcined at  $800^\circ\text{C}$  shows the typical charge curve of HT- $\text{LiCoO}_2$ . The charge curve of  $\text{LiCoO}_2$  displays a wide potential plateau near 3.9 V. Two smaller plateaus are also present at higher

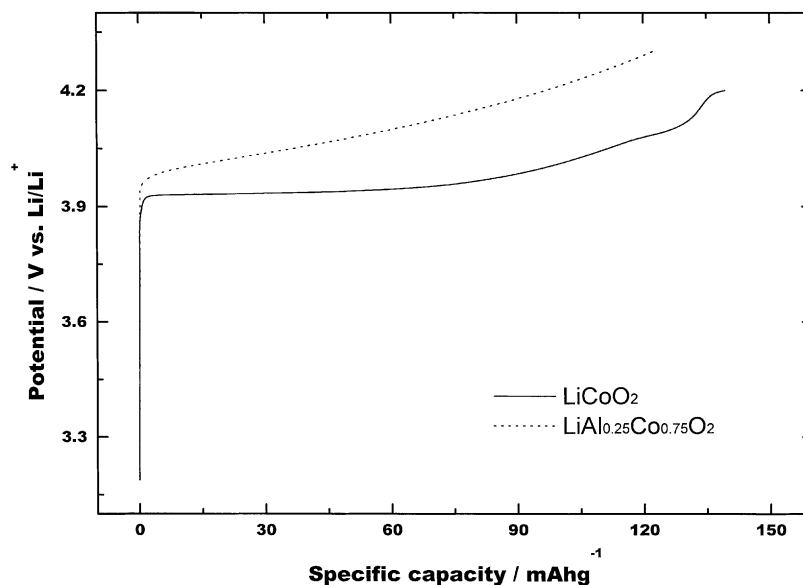


Fig. 3. First charge curves of  $\text{LiCoO}_2$  and  $\text{LiAl}_{0.25}\text{Co}_{0.75}\text{O}_2$  calcined at  $800^\circ\text{C}$  at a rate of  $C/5$ .

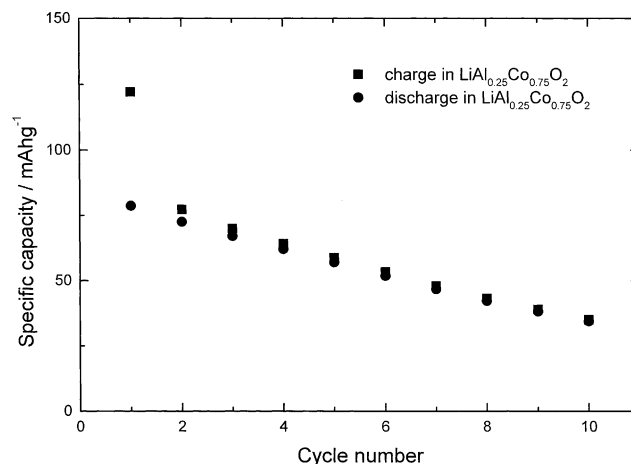


Fig. 4. Variations of specific capacity with cycling for  $\text{LiAl}_{0.25}\text{Co}_{0.75}\text{O}_2$  calcined at  $800^\circ\text{C}$  at a rate of  $C/5$  between 2.5 and 4.3 V.

potentials. The occurrence of the wide plateau near 3.9 V is due to the coexistence of two pseudo-phases of a Li-dilute  $\alpha$ -phase and an Li-concentrated  $\beta$ -phase [18]. Two smaller plateaus correspond to the order/disorder phase transition arising at around  $x = 0.5$  in the HT- $\text{Li}_{1-x}\text{CoO}_2$  [19]. On the other hand, the charge curve of  $\text{LiAl}_{0.25}\text{Co}_{0.75}\text{O}_2$  shows higher charging potential than that of  $\text{LiCoO}_2$  as predicted by the ab initio calculations [7,20]. As shown in Fig. 4,  $\text{LiAl}_{0.25}\text{Co}_{0.75}\text{O}_2$  electrode exhibits large capacity fading. After 10 cycles, the discharge capacity decreased to below 50% of the initial capacity, which should be overcome to become a good candidate of the cathode material for commercial Li rechargeable battery.

Tirado and co-workers reported with their XRD analysis that a poor lithium ion diffusivity, resulting from the presence of aluminum in both tetrahedral and octahedral sites,

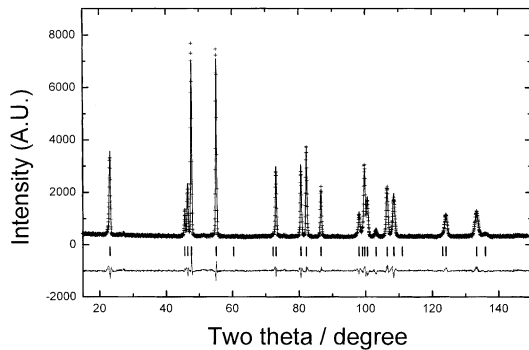


Fig. 5. Observed (+) and calculated (solid line) neutron diffraction for  $\text{LiAl}_{0.25}\text{Co}_{0.75}\text{O}_2$  calcined at  $800^\circ\text{C}$ .

may also be one of the reasons for the capacity fading of  $\text{LiAl}_{0.25}\text{Co}_{0.75}\text{O}_2$  material [4]. Fig. 5 shows neutron diffraction patterns and profile of the intensity difference between experimental and calculated neutron diffraction patterns. Rietveld refinement results of the neutron diffraction data are listed in Table 1. The Rietveld analysis of neutron diffraction patterns was carried out in the  $R\bar{3}m$  space group in order to investigate the true cation distribution. The structural parameters were refined using structural models with two different cationic distributions: (i) aluminum ions located in octahedral sites, and (ii) aluminum ions located in both tetrahedral and octahedral sites. The structural model (iii) however, led to a negative site occupation for the aluminum ions at tetrahedral sites. This indicates that aluminum and cobalt ions were statistically distributed in octahedral 3b sites. Furthermore, if aluminum ions are located in both tetrahedral and octahedral sites, the local structure of  $\text{LiAl}_{0.25}\text{Co}_{0.75}\text{O}_2$  would be greatly distorted. As shown in Fig. 2, both the edge structures of  $\text{LiCoO}_2$  and  $\text{LiAl}_{0.25}\text{Co}_{0.75}\text{O}_2$  are basically identical, and this indicates that the introduction of Al into a  $\text{LiCoO}_2$  structure does not change the local structure around Co atoms.

Fig. 6 shows XRD pattern of  $\text{LiAl}_{0.25}\text{Co}_{0.75}\text{O}_2$  electrode after 10 cycles between 2.5 and 4.3 V.  $\alpha\text{-NaFeO}_2$  structure is retained during cycling. This indicates no bulk crystalline phase change during cycling, and phase transition could be excluded from causes of capacity fading of  $\text{LiAl}_{0.25}\text{Co}_{0.75}\text{O}_2$  electrode. This is consistent with the earlier report by Jang et al., who found with their XRD analysis that the layered structure of Al-doped  $\text{LiCoO}_2$  is stable in its structure during cycling [21]. Furthermore, they reported that the variation in

Table 1  
Rietveld refinement results of the neutron diffraction data<sup>a</sup>

| Atom | Site | Occupation | x | y | z      | B ( $\text{\AA}^2$ ) |
|------|------|------------|---|---|--------|----------------------|
| Li   | 3a   | 1          | 0 | 0 | 0      | 0.714                |
| Al   | 3b   | 0.25       | 0 | 0 | 0.5    | 0.216                |
| Co   | 3b   | 0.75       | 0 | 0 | 0.5    | 0.216                |
| O    | 6c   | 2          | 0 | 0 | 0.2394 | 0.276                |

<sup>a</sup>  $a = 2.80793(11) \text{\AA}$ ,  $c = 14.11491(65) \text{\AA}$ ,  $R_{\text{wp}} = 7.33$ ,  $R_p = 5.83$ .

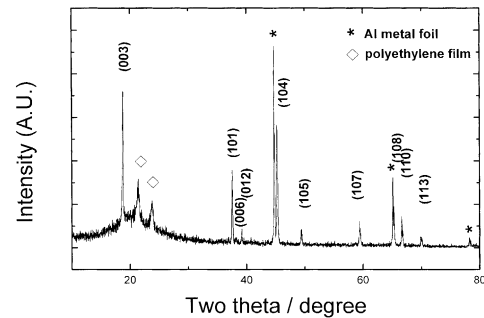


Fig. 6. XRD pattern of  $\text{LiAl}_{0.25}\text{Co}_{0.75}\text{O}_2$  electrode after 10 cycles between 2.5 and 4.3 V.

lattice constants of  $\text{LiAl}_y\text{Co}_{1-y}\text{O}_2$  during Li deintercalation is smaller than that of  $\text{LiCoO}_2$ , which indicates the lattice stabilization by Al addition. However, the XRD analysis could not explain large capacity fading of  $\text{LiAl}_y\text{Co}_{1-y}\text{O}_2$  compared to  $\text{LiCoO}_2$ . A related paper discusses the variations in the local structures with Li deintercalation and cycling process of  $\text{LiCoO}_2$  and  $\text{LiAl}_{0.25}\text{Co}_{0.75}\text{O}_2$  on the basis of XAS study, which will give a better understanding of the mechanism for the capacity fading of the  $\text{LiAl}_{0.25}\text{Co}_{0.75}\text{O}_2$  cathode during cycling process [22].

Differential scanning calorimetry (DSC) has been considered to be a useful technique to study the reactivity between active materials and the electrolyte. DSC tests were carried out in order to investigate the thermal stability of the  $\text{LiAl}_{0.25}\text{Co}_{0.75}\text{O}_2$  cathode. Fig. 7 shows DSC scans of charged cathodes containing  $\text{LiCoO}_2$  and  $\text{LiAl}_{0.25}\text{Co}_{0.75}\text{O}_2$  prepared at  $800^\circ\text{C}$ . For the pure  $\text{LiCoO}_2$  cathode, the decomposition reaction appears to initiate at around  $180^\circ\text{C}$ , followed by development of two intense exothermic peaks in the temperature range of  $200\text{--}250^\circ\text{C}$ . This is consistent with the earlier report by Zhang et al. [23]. The overall heat generation under the exothermic peaks is a direct indication of the reactivity between the active materials and the electrolyte. The thermal behavior of the

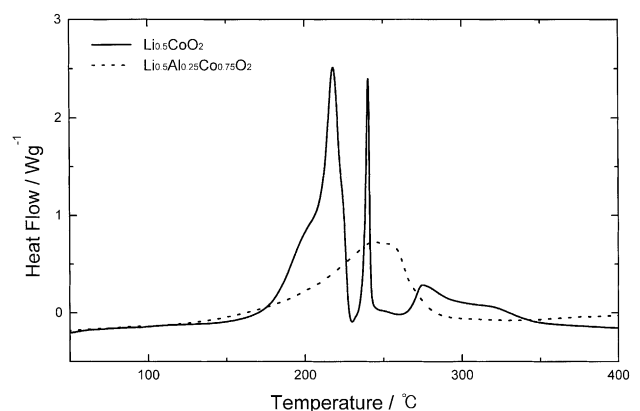


Fig. 7. DSC scans of charged cathodes containing  $\text{LiCoO}_2$  and  $\text{LiAl}_{0.25}\text{Co}_{0.75}\text{O}_2$  prepared at  $800^\circ\text{C}$ .

$\text{Li}_{0.5}\text{Al}_{0.25}\text{Co}_{0.75}\text{O}_2$  is quite different from that for  $\text{Li}_{0.5}\text{CoO}_2$ . The DSC scan of the  $\text{Li}_{0.5}\text{Al}_{0.25}\text{Co}_{0.75}\text{O}_2$  shows increase of the peak temperature and reduction of the exothermic peak compared to that of the  $\text{Li}_{0.5}\text{CoO}_2$ , which indicates that Al-doped  $\text{LiCoO}_2$  shows the good thermal stability of the cathode and reduction of the heat amount of the reaction.

#### 4. Conclusions

$\text{LiAl}_y\text{Co}_{1-y}\text{O}_2$  powders were synthesized by the sol–gel process using acrylic acid as a chelating agent. The charge curve of  $\text{LiAl}_{0.25}\text{Co}_{0.75}\text{O}_2$  showed higher charging potential than that of  $\text{LiCoO}_2$  as predicted by the ab initio calculations [7,20]. Neutron diffraction patterns and Co K-edge XANES spectra of  $\text{LiAl}_{0.25}\text{Co}_{0.75}\text{O}_2$  showed that aluminum and cobalt ions were statistically distributed in octahedral 3b sites of the ordered  $\alpha\text{-NaFeO}_2$  structure. DSC results of charged cathodes containing  $\text{LiCoO}_2$  and  $\text{LiAl}_{0.25}\text{Co}_{0.75}\text{O}_2$  showed that Al-doped  $\text{LiCoO}_2$  enhanced the thermal stability of the cathode and reduced the amount of its reaction heat with electrolyte.

#### Acknowledgements

The authors are grateful to authorities at the Pohang light source (PLS) for X-ray absorption spectroscopic measurements. This work was supported by the Brain Korea 21 project and the neutron powder diffraction experiment was carried out using HRPD at HANARO, which is operating under the Nuclear R&D Program of MOST.

#### References

- [1] K. Mizushima, P.C. Jones, P.C. Wiseman, J.B. Goodenough, *Mater. Res. Bull.* 15 (1980) 783.
- [2] T. Nagaura, K. Tozawa, *Prog. Batt. Solar Cells* 9 (1991) 209.
- [3] K. Ozawa, *Solid State Ionics* 69 (1994) 212.
- [4] R. Alcantara, P. Lavela, P.L. Relano, J.L. Tirado, E. Zhecheva, R. Stoyanova, *Inorg. Chem.* 37 (1998) 264.
- [5] M. Tabuchi, K. Ado, H. Kobayashi, H. Sakaebe, H. Kageyama, C. Masquelier, M. Yonemura, A. Hirano, R. Kanno, *J. Mater. Chem.* 9 (1999) 199.
- [6] I. Saadoune, M. Menetrier, C. Delmas, *J. Mater. Chem.* 7 (1997) 2505.
- [7] G. Ceder, Y.-M. Chiang, D.R. Sadoway, M.K. Aydinol, Y.-I. Jang, B. Huang, *Nature* 392 (1998) 694.
- [8] M. Yoshio, H. Tanaka, K. Tominaga, H. Noguchi, *J. Power Sources* 40 (1992) 347.
- [9] E. Zhecheva, R. Stoyanova, M. Gorova, R. Alcantara, J. Morales, J.L. Tirado, *Chem. Mater.* 8 (1996) 1429.
- [10] Y.K. Sun, I.H. Oh, S.A. Hong, *J. Mater. Sci.* 31 (1996) 3617.
- [11] W.-S. Yoon, K.-B. Kim, *J. Power Sources* 81/82 (1999) 517.
- [12] H.M. Rietveld, *J. Appl. Cryst.* 2 (1969) 65.
- [13] J. Rodriguez-Carvajal, *Collected Abstracts of Powder Diffraction Meeting, Toulouse, France, 1990*, p. 127.
- [14] R.J. Gummow, M.M. Thackeray, W.I.F. David, S. Hull, *Mater. Res. Bull.* 27 (1992) 327.
- [15] I.J. Pickering, G.N. George, J.T. Lewandowski, A.J. Jacobson, *J. Am. Chem. Soc.* 115 (1993) 4137.
- [16] I.J. Pickering, G.N. George, *Inorg. Chem.* 34 (1995) 3142.
- [17] M.C. Martins Alves, J.P. Dodelet, D. Guay, M. Ladouceur, G. Tourillon, *J. Phys. Chem.* 96 (1992) 10898.
- [18] Y.M. Choi, S.I. Pyun, J.S. Bae, S.I. Moon, *J. Power Sources* 56 (1995) 25.
- [19] J.N. Reimers, J.R. Dahn, *J. Electrochem. Soc.* 139 (1992) 2091.
- [20] M.K. Aydinol, A.F. Kohan, G. Ceder, K. Cho, J. Joannopoulos, *Phys. Rev. B* 56 (1997) 1354.
- [21] Y.-I. Jang, B. Huang, H. Wang, D.R. Sadoway, G. Ceder, Y.-M. Chiang, H. Liu, H. Tamura, *J. Electrochem. Soc.* 146 (1999) 862.
- [22] W.-S. Yoon, K.-K. Lee, K.-B. Kim, *J. Electrochem. Soc.*, in press.
- [23] Z. Zhang, D. Fouchard, J.R. Rea, *J. Power Sources* 70 (1998) 16.